diversity

MDPI

Article

Microclimatic Growth Rates of *Batrachochytrium salamandrivorans* under Current and Future Climates: A Very High Spatial Resolution SDM for Bsal and *Salamandra salamandra* (Linnaeus, 1758) within Forest Habitats of the European Hotspot Area

Felix Deiß [1,2], Philipp Ginal [1] and Dennis Rödder [1,*]

[1] Leibniz-Institut zur Analyse des Biodiversitätswandels (LIB), Museum Koenig, Adenauerallee 127, 53113 Bonn, Germany; f.deiss@leibniz-lib.de (F.D.); p.ginal@leibniz-lib.de (P.G.)
[2] Bundesamt für Naturschutz (BfN), Konstantinstraße 110, 53179 Bonn, Germany
* Correspondence: d.roedder@leibniz-lib.de

Abstract: Chytridiomycosis is one of the greatest threats to the diversity of amphibians worldwide. Caused by the chytrid fungus *Batrachochytrium salamandrivorans* (Bsal), it plays a decisive role in species declines. Bsal is particularly harmful to the European fire salamander (*Salamandra salamandra*), causing ulcerations, anorexia and ataxia, which ultimately lead to death. While most studies have focused on the geographic expansion of the pathogen, there is little high-resolution information available. Therefore, we chose a three-step approach in this study: We (I) used a mechanistic distribution model to project the microclimatic growth rate of Bsal within its invasive range on a spatially very high resolution (25 m). We (II) used a correlative distribution model to predict the potential distribution of *S. salamandra* and (III) applied n-dimensional hypervolumes to quantify the realized microclimatic niches of both species and examine their overlaps. We estimated future trends based on comparisons among three climate scenarios, the current microclimatic conditions and a +2 °C and +4 °C global mean temperature scenario. We demonstrated that Bsal finds suitable growth conditions everywhere within our study area, thus putting *S. salamandra* at high risk. However, climate change could lead to less suitable thermal conditions for Bsal, possibly providing a loophole for *S. salamandra*.

Keywords: chytridiomycosis; chytrid fungus; fire salamander; climate change; species distribution model; mechanistic model

Citation: Deiß, F.; Ginal, P.; Rödder, D. Microclimatic Growth Rates of *Batrachochytrium salamandrivorans* under Current and Future Climates: A Very High Spatial Resolution SDM for Bsal and *Salamandra salamandra* (Linnaeus, 1758) within Forest Habitats of the European Hotspot Area. *Diversity* **2024**, *16*, 510. https://doi.org/10.3390/d16080510

Academic Editors: James Magidi, Tsitsi Bangira and Matlhogonolo Kelepile

Received: 11 July 2024
Revised: 13 August 2024
Accepted: 20 August 2024
Published: 22 August 2024

1. Introduction

Amphibians represent the global decline of species like no other group of vertebrates, with 41% of all species facing extinction, according to the International Union for Conservation of Nature (IUCN) [1]. Besides the loss, degradation and fragmentation of habitats [2], the increased pollution of the environment [3], the appearance of invasive species [4] and climate change [5], one major threat arose from the global spread of pathogens [6]. One of these pathogens is the chytrid fungus, *Batrachochytrium salamandrivorans* (Bsal; Chytridiomycota: Rhizophydiales), which originates in Southeast Asia and most likely spread to Europe through the pet trade [7–9].

The fungus causes chytridiomycosis, particularly in salamanders and newts (Caudata), which leads to multifocal superficial erosions and deep epidermal ulcerations in the skin of infected caudata [10]. Furthermore, the animals stop eating (anorexia) and suffer from muscle spasms (ataxia), lack of interest (apathy) and skin shedding [11]. These symptoms only appear in the final stage of the disease before the hosts die within an average of 12 to 18 days after infection [12].

The European fire salamander *Salamandra salamandra* (Salamandridae) is one of the largest, native caudate amphibians within Europe and represents one of the most susceptible hosts to Bsal [7]. Its range extends across western, central, southern and southeastern Europe, from Portugal to the Carpathians and from northern Germany to southern Greece [13]. As the species depends on both aquatic and terrestrial habitats, it needs high-quality and natural habitats. In the first months, still water zones in fish-free streams, ponds and shallow water areas of mountain lakes serve as ideal larval habitats [14].

The adult animals seek damp and cool deciduous broadleaf or mixed forests in the immediate vicinity of water bodies [13]. Coniferous forests are hardly colonised, as they are usually much drier and offer fewer hiding places [15]. In addition, inland wetlands with permanent rivers, streams or creeks are very suitable habitats, too [16]. According to the authors, seasonal watercourses, peatlands, permanent or seasonal marshes, bush and herbaceous vegetation areas, as well as semi-natural gardens and urban areas, are also marginally colonised [16]. As long as there are enough retreats with a suitable microclimate, such as under piles of leaves or in old tree trunks, the salamanders can even tolerate some habitat modification [16].

These hiding places serve as brumation quarters, in which the salamanders retreat during the cold months [17], and enable the nocturnal animals to hide during the day or in unsuitable weather conditions. *Salamandra salamandra* prefers rainy nights with high humidity and temperatures ranging between 2 and 6 °C in the winter and a maximum of 20 °C during the summer months [18]. However, temperature data reported in the literature vary widely and seem to be regionally variable [19].

The first, subsequently confirmed case of Bsal in Europe dates back to 2004 when a mass mortality of *S. salamandra* occurred in Vichtbach, North Rhine-Westphalia, Germany [20]. At that time, however, the exact cause for the die-off was not yet known. In 2010, another mass mortality event was reported in the Netherlands [21], but it was not until 2013 that it became clear that these events were linked to Bsal [12]. As a result, the fire salamander populations of the Netherlands had collapsed by up to 96% and have been threatened with extinction ever since [12]. In 2014, the first cases were reported from Belgium in an area 57 km from the Dutch outbreak site [22]. Bsal then made its way to Germany, and the areas of the southern and northern Eifel, as well as the Ruhr district, represent today's hotspots [23–28]. Isolated outbreaks have even been reported in more distant areas, such as Montnegre y el Corredor National Park, Spain [29] and Ebrach, Bavaria, Germany [30]. As of today, the fungus has been detected in natural fire salamander populations in four countries, namely the Netherlands, Belgium, Germany and Spain [23–30].

Since the spread of the pathogen can quickly lead to extirpation within a susceptible host population, one of the most effective approaches seems to be the prediction of its dispersal [31]. In this regard, temperature appears to be the most important environmental variable affecting the growth of Bsal [32,33]. Bsal exhibits positive growth rates when the host's body temperature ranges between 0 °C to 25 °C, with optimal growing conditions between 10 °C and 15 °C [12], making it very well-adapted to climatic conditions in the temperate climate of central Europe [34]. Therefore, it is questionable how the fungus will respond to global warming. The IPCC Assessment Report 6 currently considers five future scenarios, namely SSP1-1.9, SSP1-2.6, SSP2-4.5, SSP3-7.0 and SSP5-8.5, suggesting an increase in the global annual mean temperature of between 1.0 °C–1.8 °C (SSP1-1.9) and 3.3 °C–5.7 °C (SSP5-8.5) [35]. As it is most likely that the 1.5 °C mark is already reached by the early 2030s [36], it might be beneficial to take climatic changes into account when estimating risks in nature conservation planning.

Since temperature regimes in micro-habitats play an important role, they can be used to model the possible spread and intensity of the pathogen by applying species distribution models (SDMs) [25]. Previous studies already predicted the potential distribution of Bsal in Europe. The correlative SDM of Lötters et al. [25] focused on its potential distribution derived from a regional climate model in Germany. However, correlative approaches only statistically link geographic occurrences with environmental data and do not necessarily

reflect species' physiological constraints [37,38]. Therefore, correlative SDM can lead to mismatches between the native and predicted invasive distribution [37,39]. Furthermore, a mechanistic SDM of Beukema et al. [34] was applied on a European scale, relying on biophysical processes such as the body temperature of the fire salamander as a host for Bsal. However, both approaches are based on broad spatial resolutions (~900 m and ~25 km, respectively), and predictions of the potential distribution of Bsal and its host on microclimatic scales are currently limited [25,34].

A microclimate is defined as the climatic conditions of a specific, small-scale area near the earth's surface [40]. These local climates have a strong influence on both plants and animals and can even affect growth and mortality rates [40]. This is especially true for ectothermic species such as fire salamanders, which regulate their body temperature through heat exchange with their environment and are therefore particularly influenced by the surrounding climate [41]. At the same time, the body temperature of salamanders influences the growth of Bsal [34].

In this study, we provide very fine-scale information on the situation in the current Bsal hotspot area (Benelux union, Germany) based on the current climate and each a +2 °C and +4 °C future global climate scenario. This information might be essential for local conservation and mitigation measurements, taking climate change into account. Therefore, we (I) applied mechanistic SDM to predict the microclimatic growth rates of Bsal on a spatially very high-resolution (25 m) within the forest habitats of the European Bsal hotspot area under current and two future climatic scenarios. Furthermore, we (II) used correlative SDMs (Maxent) to predict the potential distribution of the European fire salamander. Finally, we (III) applied n-dimensional hypervolumes to quantify the currently occupied microclimatic niches of Bsal and the fire salamander to investigate overlaps between the pathogen and its host.

2. Materials and Methods

2.1. Study Area

To determine the study area, we performed a literature review and compiled georeferenced records of all published Bsal outbreaks within Europe [12,23–28]. Due to computational limits for high-resolution modelling, we had to spatially restrict our study area. This resulted in a study area including 68 Bsal-positive localities of about 37.200 km^2 located in the border region of Germany and the Benelux. We visualised the map using Quantum GIS 3.22.8 Bialowieza (further referred to as QGIS).

Due to the low number of Bsal positive and negative records and since our microclimatic layers only cover forest habitats (see below), we used the points2nearestcell function of the rSDM package [42] to assign 16 of the 68 Bsal positive and 64 of the 369 Bsal negative records to the nearest raster cell with forest habitat. Therefore, we were able to take all records into account.

2.2. Mechanistic SDMs for Batrachochytrium salamandrivorans

Since ambient temperature determines salamander body temperature, which in turn determines Bsal growth rates [34,41], we used mapped microclimatic temperatures to (I) simulate the growth rates of Bsal under current and two future climate scenarios to investigate where it finds particularly suitable growing conditions.

We used climate layers for the current climate as well as for two future climate scenarios, assuming +2 °C and +4 °C of global warming compared to the pre-industrial climate, from the TerraClimate dataset [43]. To establish the future climate scenarios, Abatzoglou et al. [43] used monthly projections from 23 CMIP5 global climate models and downscaled them by using a pattern scaling approach [44]. The pseudo-years 1985 to 2015 served as a reference climate system, to which they applied the projected changes in temperature means and variances on a global scale in order to provide projections for the monthly climate of the future scenarios across these years.

We downloaded the monthly maximum and minimum temperatures measured 2 m above the surface in a spatial resolution of 4 km (1/24th degree) [43]. The current scenario covering the time period from 2010 to 2021 represents the history of Bsal in Europe (further referred to as current 2010–2021) [12,21–28]. As data on the two future climate scenarios are only available until 2015, we have additionally calculated the current scenario as a reference for the years 2010 to 2015 only (further referred to as current 2010–2015, future2 and future4).

We used the averages between the maximum and minimum temperatures to approximate the mean temperatures, as the microclimatic offset for forest habitats provided by Haesen et al. [45] is based on monthly means. Hence, these are necessary for the later calculation of bioclimatic variables as the TerraClimate dataset itself does not contain any information on average temperature. By applying the raster.downscale function of the spatialEco package for R [46], we downscaled the temperature layers to a 25 m resolution, using a digital elevation model (DEM) as an independent variable to account for altitude as an important determinant of temperature. We obtained the DEM via the get_dem function of the microclima package for R [47]. Based on the Bsal distribution, we cropped the layers to the forest habitats within our study area using the projectRaster function of the raster package [48]. For the coordinate reference system (CRS), we chose an equal area projection in EPSG:3035 (ETRS89-extended/LAEA Europe).

To simulate the microclimatic conditions of forest habitats, we used microclimatic temperature offset layers for the whole of European forests [45]. These layers show the average monthly offset between the microclimatic temperature in the forest and the macroclimatic temperatures in the open landscape and are provided in a resolution of 25 m for the monthly average over the years 2000 to 2021. Finally, we obtained microclimatic layers containing the mean temperatures for each month in forest habitats from 2010 to 2019. The layers were also used to correct the current 2010–2015, future2 and future4 climate scenarios for the forest microclimate at 5 cm above the ground.

For the simulation of the growth rate of Bsal, we digitised Beukemas et al.'s [34] graph of the temperature-dependent growth rate of the fungus using the digitised package for R [49]. We used these data as input for the PerfGAMM function of the Mapinguari package for R (B. Sinervo, pers. comm.) to simulate the growth rate of Bsal by applying Generalized Additive Mixed Models (GAMMs). Therefore, we projected the fitted growth rate function as estimated by the PerfGAMM function for each monthly microclimate layer translating temperatures into the growth rate of Bsal. Our simulations resulted in 146 growth rate layers for the current 2010–2021 scenario and 72 growth rate layers for each of the current 2010–2015, future2 and future4 scenarios.

We summarised the climate layers as well as the projected growth rates into meaningful units in accordance with WorldClim's bioclimatic variables [50]. Since our growth rate layers are based on monthly mean temperatures only, we created the bioclimatic variables annual mean temperature (bio1), temperature seasonality ((standard deviation $\times$ 100), bio4), mean temperature of warmest month (bio5), mean temperature of coldest month (bio6), temperature annual range (bio5–bio6), bio7), mean temperature of warmest quarter (bio10) and mean temperature of coldest quarter (bio11) [50]. In order to calculate these variables, we used the biovars function of the dismo package for R [51]. Further, we used the makeCluster function of the doParallel package for R [52] to generate these variables simultaneously, thus shortening computation time.

We generated these bioclimatic variables based on the projected monthly growth rate layers of each year for the climate scenarios current 2010–2021, current 2010–2015, future2 and future4. For these, we calculated the mean values for each variable for the respective time period considered by using the calc function of the raster package in R [51].

2.3. Correlative SDMs for S. salamandra

In the second step, we (II) predicted the potential distribution of the European fire salamander within our study area. We used the correlative SDM framework Maxent

version 3.4.0 to predict the species' distribution [53]. Maxent uses occurrence data and links them with environmental layers to predict the potential distribution of a species. We obtained 4956 occurrence records from iNaturalist (cross-linked to GBIF) and 417 records from observation.org (species records in North Rhine-Westphalia between 2010 and 2022). We used spatial filtering to subsample the species records to only one record within a 250 m radius per year to reduce potential spatial autocorrelation resulting in 502 species records for further processing. Additionally, we further reduced a potential sample bias by using a target group background approach; i.e., we used the full set of all amphibian and reptile species records within the study area excluding fire salamanders as SWD-background file in Maxent, equally filtered by a 250 m radius [54].

As environmental variables, we used the microclimatic temperature layers and elevational heterogeneity in terms of aspect, slope and the topographic wetness index (TWI) as computed in QGIS. We cropped each layer according to the forest habitats. Subsequently we calculated the Spearman rank correlation coefficient to test for multi-co-linearity between the bioclimatic variables and, based on a threshold >0.80, used only the uncorrelated variables TWI, aspect, slope, temperature seasonality (bio4), minimum temperature of the coldest month (bio6), temperature annual range (bio7), mean temperature of the warmest quarter (bio10) and mean temperature of the coldest quarter (bio11). We tested different regularization multipliers (0.5–2.5 in 0.1 steps, 5 and 10) and all feature class combinations (L = linear, P = product, Q = quadratic, H = hinge, T = threshold) in order to fit the model. For each 25 runs, we subsetted the species records into 80% used for model training and 20% used for model testing using AUC, which is a measure that indicates the overall accuracy of a model [55].

After obtaining the raw outputs of the models, we calculated the average corrected Akaike Information Criterion (AICc [56]) and the average AUC test (AUC = area under the ROC curve [57]) for each combination of settings [58]. Following Ginal et al. [58], we based our model selection on the lowest AICc and an AUC test score above 0.7. The model that explains the largest amount of variation and uses the smallest number of independent variables has the lowest AICc value and is thus chosen as the best-fitting model [59]. For the final model, we used the following combination of regularization parameters and feature classes: linear/quadratic/product features (0.050) and hinge feature (0.500). We performed 100 replicates using bootstrap, where we used a data split with 80% for model training and 20% for model testing. We applied the 10% omission threshold as presence-absence threshold based on the averaged results of the models. We utilized the Maxent Cloglog output and QGIS to create final maps.

In addition, we plotted monthly mean temperatures and relative Bsal growth rates extracted from the localities of the salamander records for the current 2010–2015, future2 and future4 scenarios.

2.4. Niche Quantification

In a third step, we (III) quantified and compared the microclimatic niches of Bsal positive and negative records as well as for the fire salamander to investigate potential overlaps of the fungus and its host. For this purpose, we used the hypervolume_svm function of the hypervolume package for R version 4.0.5 [60,61]. This algorithm applies support vector machines to separate data points from background, which reveals an n-dimensional hypervolume of the species microclimatic niche [60,62]. We used the above-mentioned species records and subset them to obtain occurrences for the fire salamander for Bsal positive and negative records. The Bsal positive and negative records also include additional samples of other caudate species (data from observation.org). It is possible that the same locality has Bsal positive and negative records in different years; however, they are associated with the relative growth rate/microclimates from that respective year. Furthermore, we sampled 10,000 random records across our study area to sample the environmental conditions.

Computation of hypervolumes requires an orthogonal niche space [58]. Hence, we used a principal component analysis (PCA) to reduce the dimensionality of the seven bioclimatic variables (bio1, bio4, bio5, bio6, bio7, bio10, bio11) to principal components (PCs). We used the princomp function of the stats package in R version 4.0.5 [61] and selected PCs with an eigenvalue $\geq$1 and calculated their explained variances and factor loadings (Table 1). In addition, we calculated values for the respective volumes of the species niches (Vol1, Vol2), the niche similarity indices of these volume ratios (Jaccard index, Sorensen index) and the proportion of the unique fraction of each hypervolume (Table 2; frac_unique1, frac_unique2).

Table 1. Summary of the principal component analysis (PCA) including factor loadings, eigenvalue and explained variance of the predicting climate variables.

Climate Parameter	Bioclimatic Variables	PC1	PC2	PC3
Annual mean temperature	bio1	0.43	0.73	0.11
Temperature seasonality	bio4	−0.89	−0.21	−0.03
Mean temperature of the warmest month	bio5	−0.33	0.63	0.59
Mean temperature of the coldest month	bio6	0.95	0.10	−0.07
Temperature annual range	bio7	−0.96	0.02	0.18
Mean temperature of warmest quarter	bio10	−0.07	0.64	−0.73
Mean temperature of coldest quarter	bio11	0.86	0.07	0.36
Eigenvalues		3.65	1.40	1.06
Explained variance		52.12	20.03	15.17

Table 2. Hypervolume statistics and comparisons among *Batrachochytrium salamandrivorans* (Bsal) positive records and the fire salamander, Bsal negative and positive records and fire salamander and random background samples. The hypervolume statistics include the respective volumes, Jaccard and Sorensen indices and the unique fractions of the respective hypervolumes.

Vol1 vs. Vol2	Vol1	Vol2	Jaccard	Sorensen	Frac_Unique_1	Frac_Unique_2
Bsal.pos vs. *S. salamandra*	24.79	75.14	0.30	0.46	0.08	0.70
Bsal.neg vs. Bsal.pos	42.04	24.79	0.54	0.70	0.45	0.06
S.salamandra vs. Background	75.14	152.89	0.47	0.64	0.03	0.53

3. Results

3.1. Microclimatic Habitat Suitability for S. salamandra and B. salamandrivorans

The topographic map, based on the DEM, reveals that the distribution of the fire salamander is associated with moderate elevations above 100 m, whereas fewer populations occur in lower elevations such as the Lower Rhine area. The Bsal positive and negative records are both predominantly located in the hotspot areas for Bsal. Our correlative SDMs reveal that under current climatic conditions, the most suitable areas for the fire salamander are located along the large streams and rivers, such as Ruhr, Rhine, Sieg, Ahr, Mosel and Maas, as well as along the Rhenish slate mountains (Figure 1A). The variables temperature seasonality (bio4, 22.6%) and slope (13.4%) were the most important variables, followed by temperature annual range (bio7, 14.7%), minimum temperature of the coldest month (bio6, 10.1%), TWI (9.4%), mean temperature of the coldest quarter (bio11, 8.5%), aspect (4.1%) and mean temperature of the warmest quarter (bio10, 3.2%). The model performance revealed a training AUC of 0.82 and a test AUC of 0.79. We have not conducted future projections of the correlative SDM, as our study area only covers a small fraction of the salamander's range; hence, future projections using a correlative approach, unlike a mechanistic one, will be likely prone to extrapolation errors.

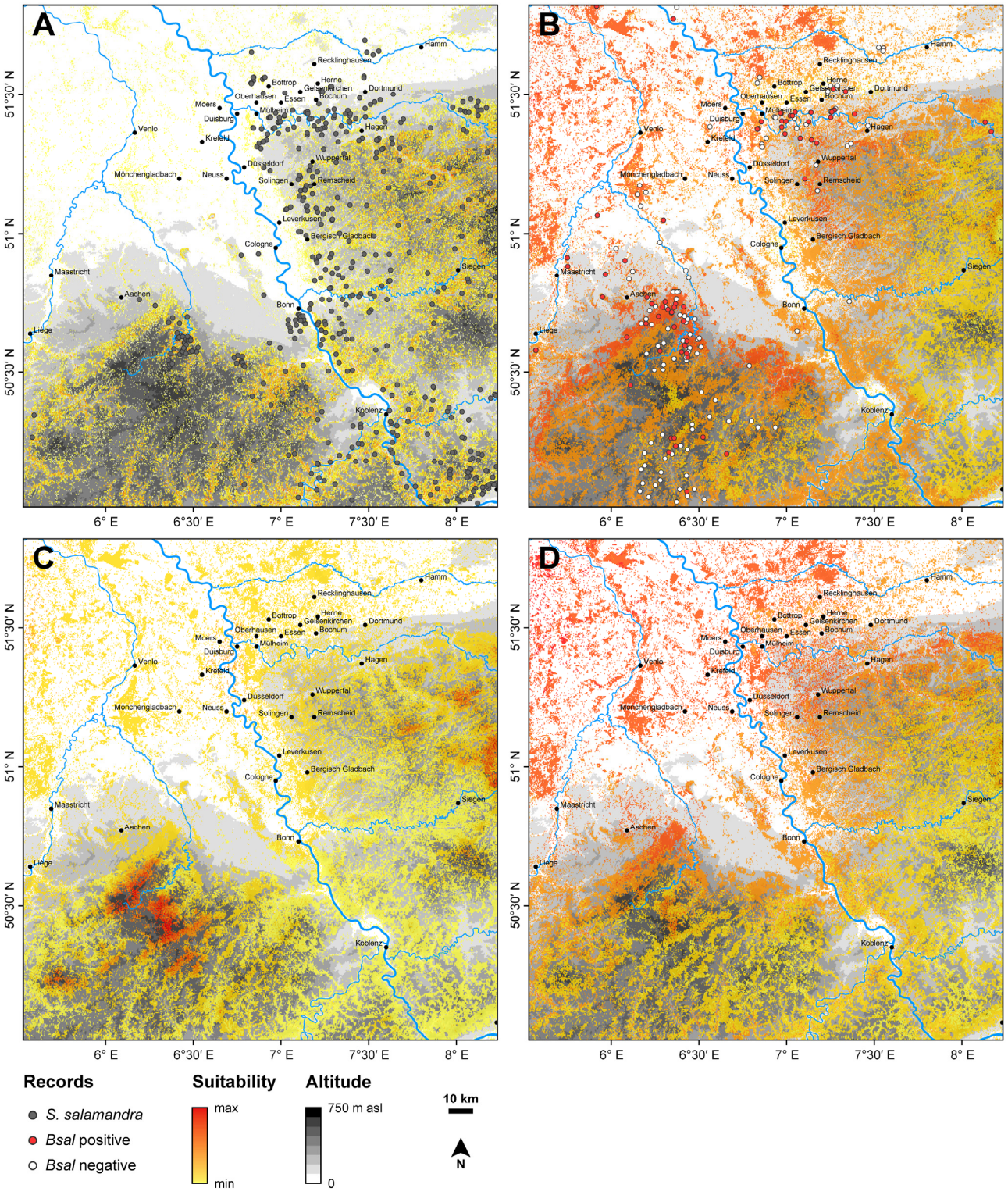

Figure 1. Performance of *Salamandra salamandra* and *Batrachochytrium salamandrivorans* (Bsal) under three climatic scenarios. Distribution of the occurrence records of *S. salamandra* combined with the Maxent results for the current climate (**A**). The annual mean microclimatic growth rates of Bsal under the current climate (**B**) and the two future climate scenarios, representing a temperature increase of +2 °C (**C**) and +4 °C (**D**). Warmer shades indicate a higher suitability for both, the occurrence of *S. salamandra* and the growth rate of Bsal (range: 2.6–4.8). For temporal variations, see Supplementary Material File S1. The map projection is EPSG:3035 (ETRS89-extended/ LAEA Europe), and a digital elevation model is added to the background of each map.

Our mechanistic SDM predicts that Bsal finds suitable growing conditions all around the year, considering the annual mean temperature (bio1) (Figure 1). We predict that Bsal can grow much better under the current climate (Figure 1B) than under the future climate scenarios of +2 °C and +4 °C (Figure 1C,D). Indeed, the fungus finds slightly better growing conditions for the +2 °C scenario than for the +4 °C scenario, especially in the Eifel region (for seasonal variations see animations in Supplementary Material File S1).

To illustrate the drastic differences in salamander distribution and fungal growth rate in relation to the different climate scenarios (current 2010–2015, future2 and future4) described above, we plotted the monthly mean temperature for each climate scenario (Figure 2A). For both the more optimistic +2 °C scenario (orange bars) and the more pessimistic +4 °C scenario (red bars), the temperatures occurring over the course of the year are increased for each single month and directly affect the growth conditions of Bsal (Figure 2B). While the relative growth of Bsal increases strongly in the colder months from November to March, it is greatly reduced in the warmer months from April to October for both the +2 °C (orange bars) and +4 °C scenarios (red bars). During midsummer, temperatures might get so high that the growth of Bsal will be close to zero. This projection is based on the digitised growth curve of Beukema et al. [34], showing the growth rate of Bsal in relation to the body temperature of the fire salamander (Figure 2C).

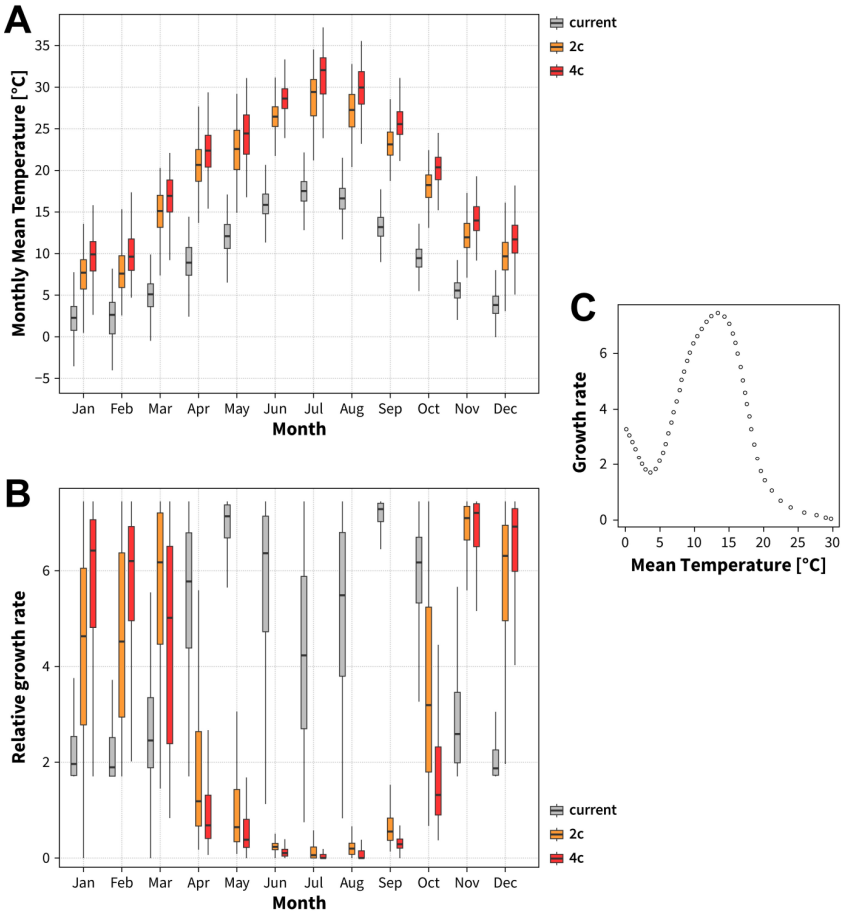

Figure 2. Growth rate of *Batrachochytrium salamandrivorans* (Bsal) with respect to the monthly mean temperature of three climatic scenarios. The figure includes the microclimatic temperature of forest habitats (**A**) with the current monthly mean temperatures (grey bars) compared to the future mean temperature for the +2 °C scenario (orange bars) and the +4 °C scenario (red bars). With respect to this microclimatic temperature, the relative growth rates of Bsal are shown (**B**) for each month for the current climate scenario (grey bars), as well as for the +2 °C (orange bars) and +4 °C (red bars) future climate scenarios, and are based on the digitised growth curve of Bsal as a function of temperature (**C**).

3.2. Niche Quantification

The PCA revealed three principal components (PCs) with an explaining variance of 87.32% (Table 1). PC1 correlates strongly with temperature seasonality (bio4), minimum temperature of the coldest month (bio6), temperature annual range (bio7) and mean temperature of the coldest quarter (bio11) and explains 52.12% of the variance. PC2 correlates strongly with annual mean temperature (bio1) and explains 20.03% of the variance. PC3 correlates strongly with the mean temperature of the warmest quarter (bio10) and explains 15.17% of the variance.

The hypervolume statistics (Table 2) reveal that the niches of Bsal positive records and the fire salamander strongly overlap, whereas the Bsal positive records are predominantly nested within the hypervolume of the fire salamander and show a much smaller niche volume (Figure 3, see also Supplementary Material File S1). The hypervolumes of Bsal positive and negative records also strongly overlap and reveal a moderate unique fraction for the negative records as well as a larger niche volume for the negative records. The comparison of the hypervolumes of the fire salamander and a hypervolume randomly sampled in the forest habitat also results in the nesting of the fire salamander niche inside the background niche revealing large overlaps between the two hypervolumes but also a large unique fraction of the background hypervolume (Table 2).

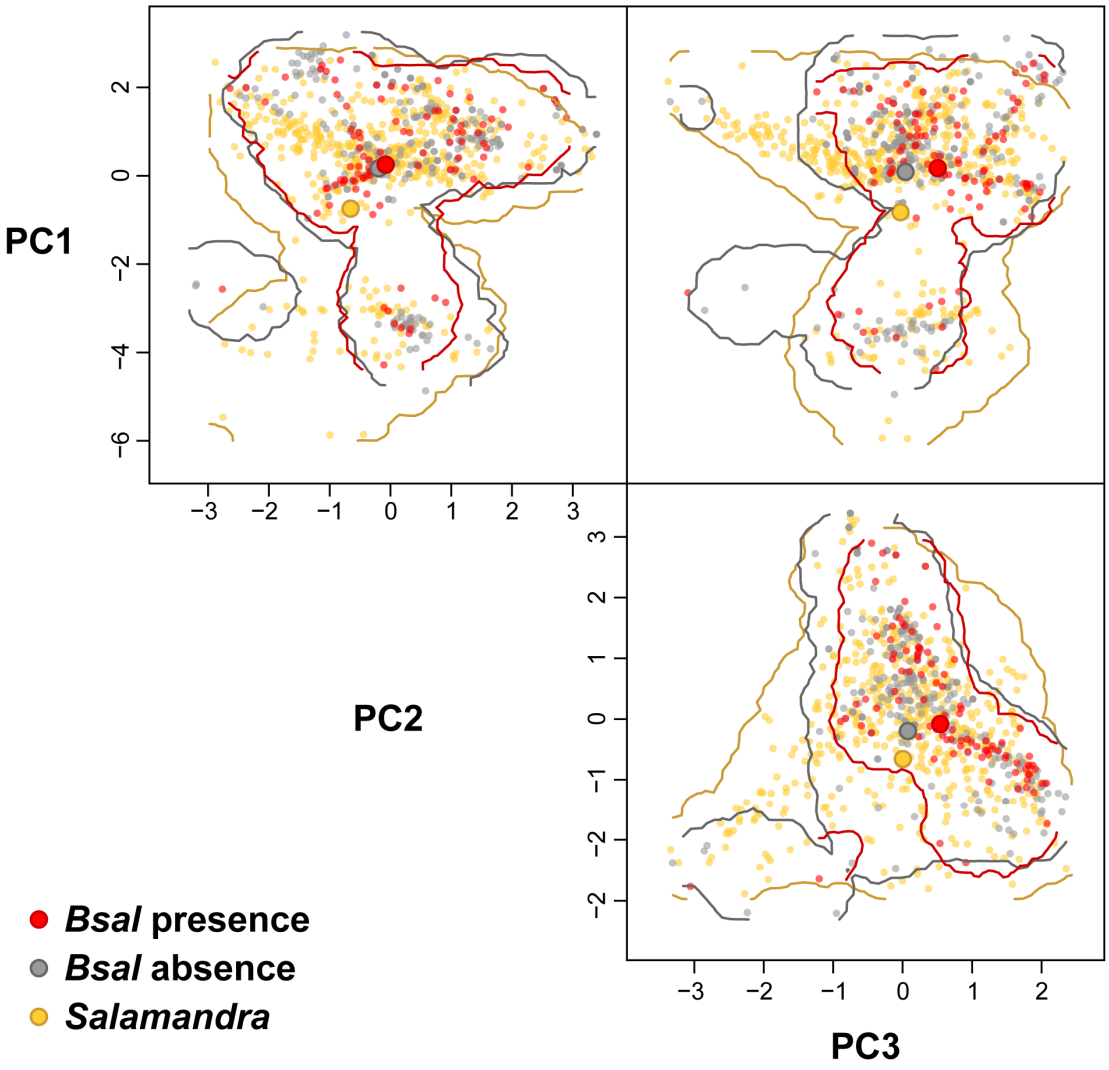

Figure 3. Comparisons among the hypervolumes of occurrences of *Salamandra salamandra* and *Batrachochytridium salamandrivorans* positive and negative localities.

4. Discussion

Our results suggest that Bsal finds suitable growth conditions throughout the whole year and everywhere within the forests of our study area. The microclimatic suitable areas within the Bsal hotspot area strongly overlap with the distribution of the fire salamander, which is also reflected in the statistics of the niche quantification. Under current climatic conditions, the highest growth rates occur during autumn (September) and spring (May), whereas the lowest growth rates are found during winter (December to February). Considering global warming scenarios of +2 °C and +4 °C, respectively, the highest growth rates for Bsal shift towards November and December, whereas the lowest growth rates will occur in summer (June to August). Hence, both global warming scenarios seem beneficial for the fire salamander in terms of Bsal infection intensities, but as future SDM projections would require extrapolation beyond the training range of the models, upper thermal limits of the salamander might be reached at some point.

4.1. Current Situation

Our mechanistic SDM reveals that Bsal finds optimal growth conditions within the European hotspot area during autumn (September) and spring (May), while only low, but still positive, growth rates occur during winter from December to February. Furthermore, the microclimatic conditions in this area seem suitable (no negative growth rates) for the fungus overall for the whole year. These findings are in accordance with the results presented by Beukema et al. [34], and it can be explained that due to the buffer capacity of the forest microclimate, caused by dense vegetation and canopy cover [63], the fungus rarely faces unsuitable climatic extremes. During summer, the leaf cover of the trees provides shade, which leads to much cooler climates than the ambient temperatures outside of forests, and during winter, the vegetation ensures reduced heat loss [63]. Consequently, animals in the forest experience a somewhat more moderate climate than their conspecifics in the open landscape [64]. Beukema et al. [34] also found that due to the nocturnal activity of host amphibians, such as the fire salamander, and the avoidance of thermal extremes, it is unlikely that Bsal exhibits temperatures above 25 °C or below 0 °C under natural conditions. These circumstances prevent effective mitigation strategies, such as behavioural fever, which is a strategy of ectothermic animals where the host deliberately seeks out warmer temperatures outside its thermal comfort zone to control its disease [34].

Considering the microclimatic niches and their quantification, we found that only a fraction of the forest habitat is microclimatically suitable for the fire salamander (Table 2; *S. salamandra* vs. background). Our correlative SDMs reveal that the occurrence of fire salamanders and high habitat suitability is associated with the valleys of rivers and streams (Figure 1A). A comparison between the Bsal positive records and the fire salamander's niches shows that the fire salamander has a large unique fraction that is not shared by Bsal yet. Similarly, the microclimatic niche of Bsal negative records also shows a unique fraction that is not shared by Bsal positive records yet. However, as our SDMs predict suitable microclimatic conditions overall for the year, and across the whole study area, we suggest that Bsal just did not spread into these areas yet, but unfortunately, we could not find any evidence for microclimatic refugia for the fire salamander in this area. Furthermore, almost the whole microclimatic niche space, where Bsal positive records are sampled, is also suitable for the fire salamander (Table 2; Bsal pos. vs. *S. salamandra* and Bsal neg. vs. Bsal pos.). This is also supported by some mass mortality events that already happened in the past, which led to collapses of some populations with mortality rates of up to 96% [12].

As geographic accessibility seems to be the only limitation for Bsal in the European hotspot area, prevention of further spread into novel areas seems to be the most effective strategy, especially in light of the rapid transmission of the fungus among susceptible hosts [65], which occurs both directly and indirectly, even through carcasses [66]. We therefore support the outlined management of Bsal according to the European Commission's Bsal-Action-Plan [67] and recommend prioritising the proposed minimisation of the risk of Bsal introduction. This includes measures such as disinfection protocols for fieldwork,

which are intended to prevent the unintentional spread of the pathogen through the use of disinfectants [67]. Accordingly, we strongly recommend that every type of field equipment (rubber boots, nets, boxes, etc.) should be thoroughly disinfected (e.g., with hydrogen peroxide or Vikron S) after visiting amphibian habitats as Bsal spreads through contaminated media too [12]. Further, the development of an Early Warning System (EWS) based on area-wide monitoring to locate new outbreaks and separate affected populations seems to be one of the most effective instruments. The EWS is supported by regional hotlines, to which citizens can report their findings, allowing for the rapid implementation of measures [67]. As suggested by the Bsal-Action-Plan, after detection, priority should be given to the reduction of the pathogen's density and the protection of the host populations [67]. Since the setup of such a system takes time, it is advisable to start monitoring in regions that are particularly at risk. As suggested by Beukema et al. [68], a southward spread of the chytrid fungus across the Ardennes and Rhineland-Palatinate seems very likely, and therefore we recommend increased efforts in these areas.

Future investigations should focus on the main dispersal pathways as well as the evaluation of methods that are undertaken. The international pet trade, for example, is an important pathway for Bsal [7]. For this reason, some countries such as the USA restricted the trade with caudate species [69]. However, these strong restrictions might also affect conservation breeding programmes negatively, as the exchange of animals is difficult or impossible. For this reason, we instead recommend the obligate testing of captive salamanders for Bsal. As the possibility of an asymptomatic infection in captive salamanders has recently been demonstrated, all captive animals should be tested, even if they appear healthy at first sight [70]. Fire salamanders that are tested positively can easily be treated with medication or by thermal treatment to cure the infection [32].

4.2. Future Scenarios

Considering global warming, under realistic (+2 °C) and extreme (+4°) conditions, we found that Bsal exhibits a shift in its maximum growth rates from September and May (current) towards November, whereas the minimum growth rates, which currently occur during the winter months (December to February) shift towards summer (June to August). Considering the thermal-dependent growth of Bsal and its thermal optimum between 10 °C and 15 °C [12,34], these seasonal shifts seem reasonable. Future work should focus on the verification of these predictions through skin swabs in high-risk areas, especially during hot summers.

It is predicted that global warming also increases the probability of weather extremes, such as extremely hot summers, which lead to droughts [71]. Generally, extremely hot and dry weather periods most likely affect Bsal as well as the fire salamander negatively [16,34]. During dry periods or brumation in winter, the salamanders retreat under deadwood piles or into abandoned underground burrows, sometimes several metres below the surface [18], which might allow for surviving these weather extremes. Possible future management actions to support fire salamander populations might therefore include habitat re-structuring, i.e., by providing cairns or piles of deadwood.

Supplementary Materials: The following supporting information can be downloaded at: https://www.mdpi.com/article/10.3390/d16080510/s1, File S1: 3D animations of the hypervolume analysis and maps of temporal variability in growth rates of *Batrachochytridium salamandrivorans* and environmental suitability for *S. salamandra*.

Author Contributions: All authors contributed to the study conception and design. The survey of Bsal records based on a literature search was carried out by F.D. Data preparation and analysis were performed by D.R. and F.D. The first draft of the manuscript was written by P.G. and F.D., and all authors commented on previous versions of this manuscript. All authors have read and agreed to the published version of the manuscript.

Funding: The authors declare that no funds, grants or other support was received during the preparation of this manuscript.

Institutional Review Board Statement: Not applicable.

Data Availability Statement: Raw data used in this study are available from the TerraClimate database (https://www.climatologylab.org/terraclimate.html, accessed on 14 October 2022).

Acknowledgments: Klaus Weddeling kindly provided data from observer.org. We are grateful for the technical support from Morris Flecks and Ursula Bott.

Conflicts of Interest: The authors have no relevant financial or non-financial interests to disclose.

References

1. IUCN Red List. Available online: https://www.iucnredlist.org/ (accessed on 12 August 2024).
2. Hammer, A.J.; McDonnell, M.J. Amphibian ecology and conservation in the urbanising world: A review. *Biol. Conserv.* **2008**, *141*, 2432–2449. [CrossRef]
3. Polo-Cavia, N.; Burraco, P.; Gomez-Mestre, I. Low levels of chemical anthropogenic pollution may threaten amphibians by impairing predator recognition. *Aquat. Toxicol.* **2016**, *172*, 30–35. [CrossRef] [PubMed]
4. Snow, N.P.; Witmer, G. American bullfrogs as invasive species: A review of the introduction, subsequent problems, management options, and future directions. *Proc. Vertebr. Pest Conf.* **2010**, *24*, 86–89. [CrossRef]
5. Blaustein, A.R.; Walls, S.C.; Bancroft, B.A.; Lawler, J.J.; Searle, C.L.; Gervasi, S.S. Direct and indirect effects of climate change on amphibian populations. *Diversity* **2010**, *2*, 281–313. [CrossRef]
6. Fu, M.; Waldman, B. Novel chytrid pathogen variants and the global amphibian pet trade. *Conserv. Biol.* **2022**, *36*, e13938. [CrossRef]
7. Martel, A.; Blooi, M.; Adriansen, C.; van Rooij, P.; Beukema, W.; Fisher, M.C.; Farrer, R.A.; Schmidt, B.R.; Tobler, U.; Goka, K.; et al. Recent introduction of a chytrid fungus endangers Western Palearctic salamanders. *Science* **2014**, *346*, 630–631. [CrossRef]
8. Laking, A.E.; Ngo, H.N.; Pasmans, F.; Martel, A.; Nguyen, T.T. *Batrachochytrium salamandrivorans* is the predominant chytrid fungus in *Vietnamese salamanders*. *Sci. Rep.* **2017**, *7*, 44443. [CrossRef]
9. Nguyen, T.T.; van Nguyen, T.; Ziegler, T.; Pasmans, F.; Martel, A. Trade in wild anurans vectors the urodelan pathogen *Batrachochytrium salamandrivorans* into Europe. *Amphib. Reptil.* **2017**, *38*, 554–556. [CrossRef]
10. Farrer, R.A. *Batrachochytrium salamandrivorans*. *Trends Microbiol.* **2019**, *27*, 892–893. [CrossRef]
11. Van Rooij, P.; Martel, A.; Haesebrouck, F.; Pasmans, F. Amphibian chytridiomycosis: A review with focus on fungus-host interactions. *J. Vet. Res.* **2015**, *46*, 137. [CrossRef]
12. Martel, A.; Spitzen-van der Sluijs, A.; Blooi, M.; Bert, W.; Ducatelle, R.; Fisher, M.C.; Woeltjes, A.; Bosman, W.; Chiers, K.; Bossuyt, F.; et al. *Batrachochytrium salamandrivorans* sp. nov. causes lethal chytridiomycosis in amphibians. *Proc. Natl. Acad. Sci. USA* **2013**, *110*, 15325–15329. [CrossRef]
13. Kwet, A. *Reptilien & Amphibien Europas*; Franckh-Kosmos Verlags-GmbH & Co. KG: Stuttgart, Germany, 2022.
14. Wagner, N.; Harms, W.; Hildebrandt, F.; Martens, A.; Ong, S.L.; Wallrich, K.; Lötters, S.; Veith, M. Do habitat preferences of European fire salamander (*Salamandra salamandra*) larvae differ among landscapes? A case study from Western Germany. *Salamandra* **2020**, *56*, 254–264.
15. Börder, M.; Karlsson, A.; Sinsch, U. Bestandsdichte, Arealnutzung und Gefährdung einer Feuersalamander-Population (*Salamandra salamandra*) im Stadtgebiet von Koblenz (Rheinland-Pfalz). *Z. Feldherp.* **2011**, *18*, 99–116.
16. IUCN Red List. IUCN SSC Amphibian Specialist Group. 2023. *Salamandra salamandra*. The IUCN Red List of Threatened Species 2023: e.T59467A219148292. Available online: https://www.iucnredlist.org/species/59467/219148292 (accessed on 6 February 2024).
17. Wilkinson, A.; Hloch, A.; Mueller-Paul, J.; Huber, L. The effect of brumation on memory retention. *Sci. Rep.* **2017**, *7*, 40079. [CrossRef] [PubMed]
18. Bogaerts, S.; Lötters, S.; Spitzen-van der Sluijs, A.; Preiβler, K.; Caspers, B.; Oswald, P.; Michaels, C.; ter Meulen, T.; Reinhardt, T.; Martel, A.; et al. *Best Practice Guidelines (Striped) Fire Salamander, Salamandra salamandra (Terrestris)*; EAZA Amphibian Taxon Advisory Group: Amsterdam, The Netherlands, 2021.
19. Catenazzi, A. Ecological implications of metabolic compensation at low temperatures in salamanders. *PeerJ* **2016**, *4*, e2072. [CrossRef]
20. Lötters, S.; Veith, M.; Wagner, N.; Martel, A.; Pasmans, F. Bsal-driven salamander mortality pre-dates the European index outbreak. *Salamandra* **2020**, *56*, 239–242.
21. Spitzen-van der Sluijs, A.; Spikmans, F.; Bosman, W.; de Zeeuw, M.; van der Meij, T.; Goverse, E.; Kik, M.; Pasmans, F.; Martel, A. Rapid enigmatic decline drives the fire salamander (*Salamandra salamandra*) to the edge of extinction in The Netherlands. *Amphib. Reptil.* **2013**, *34*, 233–239. [CrossRef]
22. Stegen, G.; Pasmans, F.; Schmidt, B.R.; Rouffaer, L.O.; van Praet, S.; Schaub, M.; Canessa, S.; Laudelout, A.; Kinet, T.; Adriaensen, C.; et al. Drivers of salamander extirpation mediated by *Batrachochytrium salamandrivorans*. *Nature* **2017**, *544*, 353–356. [CrossRef]
23. Spitzen-van der Sluijs, A.; Martel, A.; Asselberghs, J.; Bales, E.L.; Beukema, W.; Bletz, M.C.; Dalbeck, L.; Goverse, E.; Kerres, A.; Kniet, T.; et al. Expanding distribution of lethal amphibian fungus *Batrachochytrium salamandrivorans* in Europe. *Emerg. Infect. Dis.* **2016**, *22*, 1286. [CrossRef]

24. Dalbeck, L.; Düssel-Siebert, H.; Kerres, A.; Kirst, K.; Koch, A.; Lötters, S.; Ohlhoff, D.; Sabino-Pinto, J.; Preißler, K.; Schulte, U.; et al. Die Salamanderpest und ihr Erreger *Batrachochytrium salamandrivorans* (Bsal): Aktueller Stand in Deutschland. *Z. Feldherp.* **2018**, *25*, 1–22.
25. Lötters, S.; Wagner, N.; Albaladejo, G.; Böning, P.; Dalbeck, L.; Düssel, H.; Feldmeier, S.; Guschal, M.; Kirst, K.; Ohlhoff, D.; et al. The amphibian pathogen *Batrachochytrium salamandrivorans* in the hotspot of its European invasive range: Past–present–future. *Salamandra* **2020**, *56*, 173–188.
26. Schulz, V.; Schulz, A.; Klamke, M.; Preissler, K.; Sabino-Pinto, J.; Müsken, M.; Schlüpmann, M.; Heldt, L.; Kamprad, F.; Enss, J.; et al. *Batrachochytrium salamandrivorans* in the Ruhr District, Germany: History, distribution, decline dynamics and disease symptoms of the salamander plague. *Salamandra* **2020**, *56*, 189–214.
27. European Commission. Mitigating a New Infectious Disease in Salamanders to Counteract the Loss of European Biodiversity. Report, Tender ENV.B.3/SER/2016/0028, 2021. Available online: http://bsaleurope.com/wp-content/uploads/2021/03/Report_ENV.B.3-SER-2016-0028.pdf (accessed on 13 August 2024).
28. Bezirksregierung Arnsberg. Available online: https://www.bra.nrw.de/presse/massensterben-von-feuersalamandern-im-arnsberger-wald-bei-oeventrop-undfreienohl#:~:text=Im%20Bereich%20Oeventrop%20und%20Freienohl,und%20sterben%20nach%20kurzer%20Krankheitsdauer (accessed on 3 May 2022).
29. Martel, A.; Vila-Escale, M.; Fernández-Giberteau, D.; Martinez-Silvestre, A.; Canessa, S.; van Praet, S.; Pannon, P.; Chiers, K.; Ferran, A.; Kelly, M.; et al. Integral chain management of wildlife diseases. *Conserv. Lett.* **2020**, *13*, e12707. [CrossRef]
30. Bayrisches Landesamt für Umwelt. Available online: https://www.lfu.bayern.de/pressemitteilungen/c/1388268/17-20-hautpilz-bei-feuersalamander-nachgewiesen (accessed on 3 May 2022).
31. Canessa, S.; Bozzuto, C.; Campbell Grant, E.H.; Cruickshank, S.S.; Fisher, M.C.; Koella, J.C.; Lötters, S.; Martel, A.; Pasmans, F.; Scheele, B.C.; et al. Decision-making for mitigating wildlife diseases: From theory to practice for an emerging fungal pathogen of amphibians. *J. Appl. Ecol.* **2018**, *55*, 1987–1996. [CrossRef]
32. Blooi, M.; Martel, A.; Haesebrouck, F.; Vercammen, F.; Bonte, D.; Pasmans, F. Treatment of urodelans based on temperature dependent infection dynamics of *Batrachochytrium salamandrivorans*. *Sci. Rep.* **2015**, *5*, 8037. [CrossRef] [PubMed]
33. Carter, E.D.; Bletz, M.C.; le Sage, M.; la Bumbard, B.; Rollins-Smith, L.A.; Woodhams, D.C.; Miller, D.L.; Gray, M.J. Winter is coming–Temperature affects immune defenses and susceptibility to *Batrachochytrium salamandrivorans*. *PLoS Pathog.* **2021**, *17*, e1009234. [CrossRef]
34. Beukema, W.; Pasmans, F.; van Praet, S.; Ferri-Yáñez, F.; Kelly, M.; Laking, A.E.; Jesse, E.; Speybroeck, J.; Verheyen, K.; Lens, L.; et al. Microclimate limits thermal behaviour favourable to disease control in a nocturnal amphibian. *Ecol. Lett.* **2021**, *24*, 27–37. [CrossRef]
35. IPCC Sixth Assessment Report. Available online: https://www.ipcc.ch/report/ar6/wg1/ (accessed on 12 August 2024).
36. Diffenbaugh, N.S.; Barnes, E.A. Data-driven predictions of the time remaining until critical global warming thresholds are reached. *Proc. Natl. Acad. Sci. USA* **2023**, *120*, e2207183120. [CrossRef]
37. Rödder, D.; Schmidtlein, S.; Veith, M.; Lötters, S. Alien invasive Slider turtle in unpredicted habitat: A matter of niche shift or predictors studied? *PLoS ONE* **2009**, *4*, e7843. [CrossRef]
38. Fourcade, Y.; Besnard, A.G.; Secondi, J. Paintings predict the distribution of species, or the challenge of selecting environmental predictors and evaluation statistics. *Glob. Ecol. Biogeogr.* **2018**, *27*, 245–256. [CrossRef]
39. Broennimann, O.; Treier, U.A.; Müller-Schärer, H.; Thuiller, W.; Peterson, A.T.; Guisan, A. Evidence of climatic niche shift during biological invasion. *Ecol. Lett.* **2007**, *10*, 701–709. [CrossRef]
40. Naiman, R.J.; Décamps, H.; McClain, M.E.; Likens, G.E. *Riparia—Ecology, Conservation and Management of Streamside Communities*; Elsevier: Amsterdam, The Netherlands, 2005.
41. Deutsch, C.A.; Tewksbury, J.J.; Huey, R.B.; Sheldon, K.S.; Ghalambor, C.K.; Haak, D.C.; Martin, P.R. Impacts of climate warming on terrestrial ectotherms across latitude. *Proc. Natl. Acad. Sci. USA* **2008**, *105*, 6668–6672. [CrossRef]
42. Rodriguez-Sanchez, F. *rSDM: Species Distribution and Niche Modelling in R*. R Package, version 0.3.9. 2022. Available online: https://github.com/Pakillo/rSDM (accessed on 13 August 2024).
43. Abatzoglou, J.T.; Dobrowski, S.Z.; Parks, S.A.; Hegewisch, K.C. TerraClimate, a high-resolution global dataset of monthly climate and climatic water balance from 1958–2015. *Sci. Data* **2018**, *5*, 170191. [CrossRef]
44. Qin, Y.; Abatzoglou, J.T.; Siebert, S.; Huning, L.S.; AghaKouchak, A.; Mankin, J.S.; Hong, C.; Tong, D.; Davis, S.J.; Mueller, N.D. Agricultural risks from changing snowmelt. *Nat. Clim. Chang.* **2020**, *10*, 459–465. [CrossRef]
45. Haesen, S.; Lembrechts, J.J.; de Frenne, P.; Lenoir, J.; Aalto, J.; Ashcroft, M.B.; Kopecky, M.; Luoto, M.; Maclean, I.; Nijs, I.; et al. ForestTemp–Sub-canopy microclimate temperatures of European forests. *Glob. Chang. Biol.* **2021**, *27*, 6307–6319. [CrossRef]
46. Evans, T.G.; Diamond, S.E.; Kelly, M.W. Mechanistic species distribution modelling as a link between physiology and conservation. *Conserv. Physiol.* **2015**, *3*, cov056. [CrossRef]
47. Maclean, I.M.D.; Mosedale, J.R.; Bennie, J.J. Microclima: An R package for modelling meso- and microclimate. *Methods Ecol. Evol.* **2018**, *10*, 280–290. [CrossRef]
48. Hijmans, R.J.; Phillips, S.; Leathwick, J.; Elith, J. *Dismo: Species Distribution Modeling*. R Package, Version 1.3-9. 2022. Available online: https://CRAN.R-project.org/package=dismo (accessed on 13 August 2024).
49. Poisot, T. The digitize package: Extracting numerical data from scatterplots. *R J.* **2011**, *3*, 25–26. [CrossRef]

50. Hijmans, R.J.; Cameron, S.E.; Parra, J.L.; Jones, P.G.; Jarvis, A. Very high resolution interpolated climate surfaces for global land areas. *Int. J. Climatol.* **2005**, *25*, 1965–1978. [CrossRef]
51. Hijmans, R.J. *Raster: Geographic Data Analysis and Modelling with Raster Data*. R Package, Version 3.5-29. 2022. Available online: https://CRAN.R-project.org/package=raster (accessed on 13 August 2024).
52. Folashade, D.; Microsoft Corporation; Weston, S.; Tenenbaum, D. *DoParallel: Foreach Parallel Adaptor for the 'Parallel' Package*. R Package, Version 1.0.17. 2022. Available online: https://CRAN.R-project.org/package=doParallel (accessed on 13 August 2024).
53. Phillips, S.J.; Anderson, R.P.; Schapire, R.E. Maximum entropy modeling of species geographic distributions. *Ecol. Model.* **2006**, *190*, 231–259. [CrossRef]
54. Barber, R.A.; Ball, S.G.; Morris, R.K.; Gilbert, F. Target-group backgrounds prove effective at correcting sampling bias in Maxent models. *Divers. Distrib.* **2022**, *28*, 128–141. [CrossRef]
55. Mandrekar, J.N. Receiver operating characteristic curve in diagnostic test assessment. *J. Thorac. Oncol.* **2010**, *5*, 1315–1316. [CrossRef] [PubMed]
56. Warren, D.L.; Seifert, S.N. Ecological niche modeling in Maxent: The importance of model complexity and the performance of model selection criteria. *Ecol. Appl.* **2011**, *21*, 335–342. [CrossRef] [PubMed]
57. Phillips, S.J. A brief tutorial on Maxent. *ATT Res.* **2005**, *190*, 231–259.
58. Ginal, P.; Tan, W.C.; Rödder, D. Invasive risk assessment and expansion of the realized niche of the Oriental Garden Lizard *Calotes versicolor* species complex (Daudin, 1802). *Front. Biogeogr.* **2022**, *14*, e54299. [CrossRef]
59. Cavanaugh, J.E.; Neath, A.A. The Akaike information criterion: Background, derivation, properties, application, interpretation, and refinements. *Wiley Interdiscip. Rev. Comput. Stat.* **2019**, *11*, e1460. [CrossRef]
60. Blonder, B.; Morrow, C.B.; Harris, D.J.; Brown, S.; Butruille, G.; Laini, A.; Chen, D. *Hypervolume: High Dimensional Geometry, Set Operations, Projection, and Inference Using Kernel Density Estimation, Support Vector Machines, and Convex Hulls*. R Package, Version 3.1.0.. 2022. Available online: https://cran.r-project.org/web/packages/hypervolume/hypervolume.pdf (accessed on 13 August 2024).
61. R Core Team. *R: A Language and Environment for Statistical Computing*; R Foundation for Statistical Computing: Vienna, Austria, 2021.
62. Blonder, B.; Lamanna, C.; Violle, C.; Enquist, B.J. The n-dimensional hypervolume. *Glob. Ecol. Biogeogr.* **2014**, *23*, 595–609. [CrossRef]
63. De Frenne, P.; Lenoir, J.; Luoto, M.; Scheffers, B.R.; Zellweger, F.; Aalto, J.; Ashcroft, M.B.; Christiansen, D.M.; Decocq, G.; de Pauw, K.; et al. Forest microclimates and climate change: Importance, drivers and future research agenda. *Glob. Chang. Biol.* **2021**, *27*, 2279–2297. [CrossRef]
64. Kearney, M.; Shine, R.; Porter, W.P. The potential for behavioral thermoregulation to buffer "cold-blooded" animals against climate warming. *Proc. Natl. Acad. Sci. USA* **2009**, *106*, 3835–3840. [CrossRef]
65. Malagon, D.A.; Melara, L.A.; Prosper, O.F.; Lenhart, S.; Carter, E.D.; Fordyce, J.A.; Peterson, A.C.; Miller, D.L.; Gray, M.J. Host density and habitat structure influence host contact rates and *Batrachochytrium salamandrivorans* transmission. *Sci. Rep.* **2020**, *10*, 5584. [CrossRef]
66. Carter, E.D.; DeMarchi, J.A.; Wilber, M.Q.; Miller, D.L.; Gray, M.J. *Batrachochytrium salamandrivorans* is necronotic: Carcasses could play a role in Bsal transmission. *Front. Amphib. Reptile Sci.* **2024**, *2*, 1284608. [CrossRef]
67. Gilbert, M.J.; Spitzen-van der Sluijs, A.; Canessa, F.; Bosch, J.; Cunningham, A.; Grasselli, E.; Laudelout, A.; Lötters, S.; Miaud, C.; Salvidio, S.; et al. Mitigating *Batrachochytrium salamandrivorans* in Europe. In *Batrachochytrium salamandrivorans Action Plan for European Urodeles*; European Commission: Nijmegen, The Netherlands, 2020.
68. Beukema, W.; Erens, J.; Schulz, V.; Stegen, G.; Spitzen-van der Sluijs, A.; Stark, T.; Laudelout, A.; Kinet, T.; Kirschey, T.; Poulain, M.; et al. Landscape epidemiology of *Batrachochytrium salamandrivorans*: Reconciling data limitations and conservation urgency. *Ecol. Appl.* **2021**, *31*, e02342. [CrossRef] [PubMed]
69. Yap, T.A.; Nguyen, N.T.; Serr, M.; Shepack, A.; Vredenburg, V.T. *Batrachochytrium salamandrivorans* and the risk of a second amphibian pandemic. *EcoHealth* **2017**, *14*, 851–864. [CrossRef] [PubMed]
70. Sabino-Pinto, J.; Veith, M.; Vences, M.; Steinfartz, S. Asymptomatic infection of the fungal pathogen *Batrachochytrium salamandrivorans* in captivity. *Sci. Rep.* **2018**, *8*, 11767. [CrossRef]
71. Vicente-Serrano, S.M.; Quiring, S.M.; Pena-Gallardo, M.; Yuan, S.; Dominguez-Castro, F. A review of environmental droughts: Increased risk under global warming? *Earth Sci. Rev.* **2020**, *201*, 102953. [CrossRef]